The Fe(III), Co(III), and V(III) Complexes of the "Heteroscorpionate" Ligand (2-Thiophenyl)bis(pyrazolyl)methane

Timothy C. Higgs,[†] David Ji,[‡] Roman S. Czernuszewicz,[‡] Berthold F. Matzanke,[||] Volker Schunemann,[||] Alfred X. Trautwein,[||] Madeleine Helliwell,[§] Wilfredo Ramirez,[†] and Carl J. Carrano*,[†]

Departments of Chemistry, Southwest Texas State University, San Marcos, Texas 78666, University of Houston, Houston, Texas, 77204, The University of Manchester, Oxford Road, Manchester, M13 9PL, England, and The Institute for Physics, Medical University of Lübeck, D-23538 Lübeck, Germany

Received September 5, 1997

The synthesis and characterization of the tridentate "heteroscorpionate" mixed functionality ligand, (2-thiophenyl)-bis(pyrazolyl)methane, L1, is reported. This ligand was used to synthesize the complexes, $[Fe(L1)_2][ClO_4]$, $[Co(L1)_2][BPh_4]$, and $[V(L1)_2][BPh_4]$. X-ray crystallographic analysis of the latter two complexes gave the following structural parameters: $[V(L1)_2][BPh_4]\cdot MeCN\cdot {}^{i}Pr_2O$, $C_{58}H_{57}N_9B_1O_1S_2V_1$, monoclinic, $a = 16.197(2)$ Å, $b = 19.281(2)$ Å, $c = 17.985(2)$ Å, $\beta = 102.343(9)°$, space group $P2_1/c$; $[Co(L1)_2][BPh_4]\cdot CH_2Cl_2$, $C_{51}H_{42}N_8B_1Cl_2Co_1S_2$, triclinic, $a = 12.751(1)$ Å, $b = 12.830(1)$ Å, $c = 14.740(1)$ Å, $\alpha = 98.351(7)°$, $\beta = 98.122(6)°$, $\gamma = 97.023(8)°$, space group $P\bar{1}$. An example of the use of this new class of "heteroscorpionate" ligands for systematic comparisons of electronic properties of metal complexes with identical topology that vary only in the nature of one of the donor atoms is given.

Introduction

Mixed nitrogen−sulfur coordination of transition metals is a widely observed motif in biochemistry appearing in metalloproteins such as the "zinc-fingers", cupredoxins, isopenicillin-*N*-synthase, and Reiske centers.[1] Other more recently described examples are the nitrile hydratases which are bacterial enzymes that catalyze the hydration of nitriles to amides. Two basic types of this enzyme are known, one isolated from various species of *Rhodococcus* sp. and *Pseudomonas chlororaphis* which contain non-heme iron in their active sites[2] and another isolated from *Rhodococcus rhodochrous* which contains noncorrin cobalt.[3] Both enzymes are used industrially in Japan to produce acrylamide from acrylonitrile and nicotinamide from 3-cyano-pyridine.[4] The recent crystal structure of the iron-containing enzyme reveals an unprecedented structure with the iron bound to three cysteine sulfurs and two peptide nitrogens, giving a pseudo-square-pyramidal five-coordinate geometry.[5] Various spectroscopic techniques indicate that the iron in the enzyme is low spin.[6,7] Although much less is known about the cobalt enzyme, recent studies suggest a low-spin Co(III) ion bound to a site virtually identical to that found for the iron.[8] This would make it the only known example of a non-corrin Co(III) enzyme as well as the only example of biological Co−S coordination. From an inorganic chemist's perspective there is much about these enzymes that is intriguing. In particular, why has nature chosen binding sites for these metal ions which force upon them the low-spin configuration, since low-spin Fe(III) and Co(III) are normally considered "kinetically inert" ions which would seem to preclude their use as catalytic centers (where kinetic lability is generally the rule).

The interaction of vanadium with sulfur ligands also appears in many biological systems such as the nitrogenases[9] and has been implicated in its reactions with glutathione[10] and in the mechanism of action of vanadium containing insulin mimetic compounds.[11] Finally, there is an industrial significance to V−S interactions, centered around the need to better understand the nature of the species involved in the poisoning of the vanadium hydrodesulfurization catalysts used in crude oil processing.[12]

To address many of these issues, we and others have begun to study model complexes of Fe(III), V(III), and Co(III) where the metal is coordinated in a fashion similar to that predicted to occur in the enzymes and other systems and to study their spectroscopic, electronic, and structural characteristics.[13−16] To

* Corresponding author.
[†] Southwest Texas State University.
[‡] University of Houston.
[§] University of Manchester.
[||] Medical University of Lübeck.

(1) Holm, R. H.; Kennepohl, P.; Solomon, E. I. *Chem. Rev.* **1996**, *96*, 2239.
(2) Nagasawa, T.; Ryuno, K.; Yamada, H. *Biochem. Biophys. Res. Commun.* **1986**, *139*, 1305.
(3) Nagasawa, T.; Takeuchi, K.; Yamada, H. *Biochem. Biophys. Res. Commun.* **1988**, *155*, 1008.
(4) Komeda, H.; Kobayashi, M.; Shimizu, S. *Proc. Natl. Acad. Sci. U.S.A.* **1997**, *94*, 36.
(5) Huang, W.; Jia, J.; Cummings, J.; Nelson, M.; Schneider, G.; Lindquist, Y. *Structure* **1997**, *5*, 691.
(6) Sugiura, Y.; Kuwahara, J.; Nagasawa, T.; Yamada, H. *J. Am. Chem. Soc.* **1987**, *109*, 5848.
(7) Scarrow, R. C.; Brennen, B. A.; Cummings, J. G.; Jin, H.; Duong, D. J.; Kindt, J. T.; Nelson, M. J. *Biochemistry* **1996**, *35*, 10078.
(8) Brennan, B. A.; Alms, G.; Nelson, M. J.; Durney, L. T.; Scarrow, R. C. *J. Am. Chem. Soc.* **1996**, *118*, 9194.
(9) Eady, R. R. In *Metal Ions in Biological Systems*; Sigel, H., and Sigel, A., Eds.; Marcel Dekker: New York, 1995; Vol. 31, p 363.
(10) Thompson, W. J.; Tan, B. H.; Strada, S. J. *J. Biol. Chem.* **1991**, *266*, 17011.
(11) Huyer, G.; Liu, S.; Kelley, J.; Moffat, J.; Payette, P.; Kennedy, B.; Tsaprailis, G.; Gresser, M. J.; Ramachandran, C. *J. Biol. Chem.* **1997**, *272*, 843.
(12) Reynolds, J. G.; Gallegos, E. J.; Fish, R. H.; Komlenic, J. *Energy Fuels* **1987**, *1*, 36.

S0020-1669(97)01151-8 CCC: $15.00
Published on Web 04/14/1998

this end we have utilized a thiolate-containing member of a new class of "heteroscorpionate" ligand, and we have already studied the coordination characteristics of the phenolate analogue with Ni(II), Co(II), and Cu(II).[17−19] Herein we describe the synthesis of this new ligand, (2-thiophenyl)bis(pyrazolyl)methane, and report its coordination properties with the trivalent cations of Fe, Co, and V.

Experimental Procedures

All operations were carried out in air unless otherwise stated, and the solvents used were of reagent grade or better (Aldrich Chemical Co.). Anhydrous THF was dried over sodium/benzophenone, while MeCN was dried and distilled over CaH_2. Microanalyses were performed by Desert Analytics Laboratory (Tucson, AZ). For ^{1}H and ^{13}C NMR spectroscopy, we utilized either an IBM Instruments 80 MHz or a Varian INOVA 400 MHz FT-NMR system. IR spectra were recorded either as evaporated films on NaCl plates or via KBr disks on a Perkin-Elmer 1600 series FT-IR. Solid-state magnetic measurements were performed on a Johnson-Matthey susceptibility balance. Solution electronic spectra were obtained on a Hewlett-Packard 8452A diode array spectrophotometer under the computer control of a PC with OLIS diode array spectrophotometry software (On-Line Instruments, Inc.). Cyclic voltammetry data were acquired in acetonitrile solution using a Bioanalytical Systems, Inc. CV-50W voltammetric analyzer system (consisting of a CV-50W potentiostat and C2 cell stand) under PC computer control with platinum working and secondary electrodes, a BAS SCE reference, and [^{n}Bu$_4$N][PF$_6$] as supporting electrolyte. Ferrocene was used as an internal standard and exhibits an oxidation potential of +452 mv under these conditions. Resonance Raman spectra were acquired by excitation with discrete lines from Coherent 90-6 Ar^+ (457.9−514.5 nm) and K-2 Kr^+ (406.7−676.4 nm) ion lasers. The scattered photons were collected via backscattering from spinning solid samples in pressed KCl pellets[20] or spinning MeCN solutions in NMR tubes. A scanning Raman instrument equipped with a Spex 1403 double monochromator and a Hamamatsu 928 photomultiplier detector system was used to record the spectra under control of a Spex DM3000 microcomputer system as described elsewhere.[21] On average, three to five multiple scans were taken to improve the signal-to-noise ratio. Raman data manipulation was preformed using LabCalc software (Galactic Industries Inc.). Excitation profiles were obtained by recording solid-state Raman spectra of a sample mixed with K_2SO_4 as an internal standard. The 986 cm^{-1} peak of the sulfate totally symmetric vibrational mode was used for measurement of relative intensities.

Synthesis of Ligand L1. 2-Aminobenzaldehyde was prepared by the reduction of 2-nitrobenzaldehyde with ferrous sulfate as described by Smith and Opie.[22] ^{1}H NMR (80 MHz, $CDCl_3$): δ 6.11 (bs, NH_2, 2H), 6.58−6.83 (m, ArH, 2H), 7.2−7.53 (m, ArH, 2H), 9.87 (s, ArCHO, 1H).

2-Thiocyanatobenzaldehyde was synthesized by preparation of the diazonium salt of 2-aminobenzaldehyde with $NaNO_2/H_2SO_4$ followed by immediate reaction in situ with CuSCN and a large excess of KSCN as described by West et al.[23] ^{1}H NMR (80 MHz, $CDCl_3$): δ 7.26 (s, $CHCl_3$), 7.45−7.98 (m, ArH, 4H), 10.04 (s, ArCHO, 1H). IR (evap. film; NaCl plate, cm^{-1}): 2863, 2164, 1677, 1587, 1562, 1462, 1442, 1398, 1303, 1268, 1218, 1063, 858, 758, 678, 653.

(2-Thiocyanatophenyl)bis(pyrazolyl)methane. Bis(pyrazolyl)ketone (8.084 g, 0.0499 mol), 2-thiocyanatobenzaldehyde (8.1364 g, 0.0499 mol), and anhydrous $CoCl_2$ (0.08 g, 0.616 mmol) were placed together in a 100 cm^3 round-bottom flask. The contents of the flask were thoroughly mixed, and the flask purge-filled with argon three times. The reaction mixture was then heated to 85 °C, under vigorous magnetic stirring. As the flask was heated its contents melted and a vigorous effervescence due to CO_2 evolution was observed, which subsided after about 60 s. The mixture changed color during the course of the reaction from green to pink to brown to dark brown over a period of 25 min. After this time, the reaction mixture was allowed to cool to room temperature and the resultant dark brown oil dissolved in CH_2Cl_2 (50 cm^3). The CH_2Cl_2 solution was extracted with two portions of distilled water (2 × 50 cm^3), and the organic layer was separated and dried over $MgSO_4$ for 45 min. After drying, the CH_2Cl_2 was evaporated under reduced pressure to yield a dark brown oil. The oil was dissolved in Et_2O (50 cm^3), and the solution cooled to −78 °C via a dry ice/acetone bath for 30 min. The solution was then filtered, removing a small amount of an intense purple solid. The volume of the ethereal filtrate was halved by evaporation under a reduced pressure. This more concentrated solution was then cooled again to −78 °C, and the sides of the flask were vigorously scratched with a glass rod which induced the deposition of a microcrystalline solid. The solution was kept at −78 °C for 1 h before the solid was collected by filtration, washed with Et_2O (2 × 10 cm^3 portions), and dried in vacuo to yield a very pale purple microcrystalline solid. Yield: 8.4 g (59.9%). ^{1}H NMR (80 MHz, $CDCl_3$): δ 6.37 (t, 4-pzH, 2H), 6.70−6.96 (m, ArH, 1H), 7.26 (s, $CHCl_3$), 7.32−7.88 (m, ArH (3H) + 3-pzH (2H) + 5-pzH (2H)), 7.93 (s, ArCHO, 1H). IR (evap. film; NaCl plate, cm^{-1}): 3112, 2153, 1518, 1467, 1435, 1389, 1311, 1200, 1085, 1043, 965, 849, 799, 748, 628.

(2-Thiophenyl)bis(pyrazolyl)methane, L1. (2-Thiocyanatophenyl)-bis(pyrazolyl)methane (2.266 g, 8.063 × 10^{-4} mol) was dissolved in anhydrous THF (20 cm^3) under an argon atmosphere. Separately, $LiAlH_4$ in THF solution (12.9 cm^3, 1.0 M in THF) was transferred by syringe to a 100 cm^3 three-necked round-bottomed flask equipped with a reflux condenser that had been purged with argon. The (2-thiocyanatophenyl) bis(pyrazolyl)methane in THF solution was then added dropwise (*carefully*!!) to the $LiAlH_4$ solution via syringe. This addition was accompanied by vigorous effervescence. After the completion of this addition, the reaction mixture was refluxed for 1 h. The apparatus was then allowed to cool to room temperature before being immersed in an ice/water bath (while the reaction mixture was maintained under argon) and cooled to 3 °C. Aqueous NaOH (10 cm^3 of a 10% solution) was added to the reaction mixture over the course of 30 min (*Caution! Exothermic hydrogen evolution*!) in a dropwise fashion via syringe. Once all the excess $LiAlH_4$ had been destroyed the mixture was filtered to remove the resultant polymeric $Al(OH)_3$ which was washed with water. The filtrates were combined and rotary evaporated to remove most of the THF component of the mixture, leaving a deep yellow aqueous solution containing lithium [2-thiolatophenylbis(pyrazolyl)-methane]. The aqueous solution was then neutralized to pH 5 using 6 N H_2SO_4 (aq) which caused a lightening of the deep yellow solution and deposition of some yellow oil. The mixture was extracted with CH_2Cl_2 (2 × 100 cm^3), and the organic layers were combined and dried over $MgSO_4$ for 45 min. The CH_2Cl_2 solution was then evaporated to dryness under reduced pressure yielding a yellow oil. Hexane (15 cm^3) and ^{i}Pr$_2$O (not more than 10 drops) were added to the oil which was then scratched vigorously with a glass rod to effect its trituration to a pale yellow solid which was stored under argon to prevent aerial oxidation to disulfide. Yield: 1.6−1.9 g (72−86%). ^{1}H NMR (80 MHz, $CDCl_3$): δ 3.11 (s, ArSH, 1H), 6.28 (t, 4-pzH, 2H), 6.65 (m, ArH, 1H), 7.0−7.42 (m, ArH (3H) + 5-pzH (2H)), 7.59 (d, 3-pzH, 2H), 7.87 (s, CH, 1H). IR (evap. film; NaCl plate, cm^{-1}): 3112, 3063, 2926, 2506, 1588, 1509, 1471, 1432, 1388, 1309, 1251, 1217, 1197, 1085, 1046, 967, 918, 854, 826, 800, 747, 631.

[V(L1)$_2$][BPh$_4$], 2. L1 (0.20 g, 7.298 × 10^{-4} mol) and NaOMe (0.0394 g, 7.298 × 10^{-4} mol) were dissolved in anhydrous degassed

(13) Nivorozhkin, A. L.; Uraev, A. I.; Bondarenko, G. I.; Antsyshkina, A. S.; Kurbatov, V. P.; Garnovskii, A. D.; Turta, C. I.; Brashoveanu, N. D. *Chem. Commun.* **1997**, 1711.
(14) Sakurai, H.; Tsuchiya, K.; Migita, K. *Inorg. Chem.* **1988**, *27*, 3879.
(15) Shoner, S. C.; Barnhart, D.; Kovacs, J. A. *Inorg. Chem.* **1995**, *34*, 4517.
(16) Beissel, T.; Beurger, K. S.; Voigt, G.; Weighardt, K., Butzlaff, C.; Trautwein, A. X. *Inorg. Chem.* **1993**, *32*, 124.
(17) Higgs, T. C.; Carrano, C. J. *Inorg. Chem.* **1997**, *36*, 291.
(18) Higgs, T. C.; Carrano, C. J. *Inorg. Chem.* **1997**, *36*, 298.
(19) Higgs, T. C.; Ji, D.; Czernuscewicz, R. S.; Carrano, C. J. *Inorg. Chim. Acta* **1998**, in press.
(20) Czernuszewicz, R. S. *Appl. Spectrosc.* **1986**, *40*, 571.
(21) Czernuszewicz, R. S. In *Methods in Molecular Biology*; Jones, C., Mulloy, B., Thomas, A. H., Eds.; Humana Press: Totowa, NJ, 1993; Vol. 17, pp 345−374.
(22) Smith, L. I.; Opie, J. W. *Organic Syntheses. Collective Volume 3*, Wiley: London, 1955; p 56.
(23) Marini, P. J.; Murray, K. S.; West, B. O. *J. Chem. Soc., Dalton Trans.* **1983**, 143.

Table 1. Crystallographic Data and Data Collection Parameters for $[V(L1)_2][BPh_4]\cdot MeCN\cdot {}^iPr_2O$ and $[Co(L1)_2][BPh_4]\cdot CH_2Cl_2$

	$[V(L1)_2][BPh_4]\cdot MeCN\cdot {}^iPr_2O$	$[Co(L1)_2][BPh_4]\cdot CH_2Cl_2$
empirical formula	$C_{58}H_{57}N_9B_1O_1S_2V_1$	$C_{51}H_{42}N_8B_1Cl_2Co_1S_2$
space group	$P2_1/c$	$P\bar{1}$
temperature, K	298	298
a, Å	16.197(2)	12.751(1)
b, Å	19.281(2)	12.830(1)
c, Å	17.985(2)	14.740(1)
α, deg		98.351(7)
β, deg	102.343(9)	98.122(6)
γ, deg		97.023(8)
V, Å^3	5486.9(14)	2336.70(43)
ρ, g cm^{-3}	1.237	1.381
Z	4	2
fw	1022.0	971.7
crystal size, mm	0.7 × 0.7 × 0.2	0.5 × 0.4 × 0.2
crystal color, habit	dark blue, plate	green-brown, block
μ, mm^{-1}	0.305	0.617
radiation	Mo Kα	Mo Kα
scan type	$\theta-2\theta$	$\theta-2\theta$
data collection range, deg.	3.5−40.0	3.5−45.0
no. of unique data	5065	6052
no. of obsd data	3276 ($F > 2\sigma(F)$)	4211 ($F > 4\sigma(F)$)
data:parameter ratio	6:1	6.8:1
transmission factors	−	0.8265/1.0000
R^a	8.74	4.15
$R_w{}^a$	8.38	4.91
max difference peak, eÅ^{-3}	+0.49	−0.27
Δ/σ(avg)	0.005	0.012

[a] Quantity-minimized $\omega w(F_o - F_c)^2$. $R = \Sigma|F_o - F_c|/\omega F_o$. $R_w = (\omega w(F_o - F_c)^2/\Sigma(\omega F_o)^2)^{1/2}$.

MeCN (10 cm^3) under an argon atmosphere. Separately $VCl_3\cdot 3THF$ (0.136 g, 3.649 × 10^{-4} mol) and $NaBPh_4$ (0.125 g, 3.649 × 10^{-4} mol) were dissolved in anhydrous degassed MeCN (10 cm^3) under argon. The NaL1 solution was then transferred by cannula into the $VCl_3\cdot 3THF/NaBPh_4$ solution, causing an instant color change from red/pink to a very intense blue color. The reaction mixture was stirred for 30 min at room temperature before the solution was evaporated to a volume of about 5 cm^3 under reduced pressure. The reaction mixture was then cannula filtered into a 25 cm^3 Schlenk tube under argon, and the solution was layered with degassed $^iPr_2O$ (15 cm^3). Over a period of weeks, blue block-like crystals appeared on the side of the Schlenk tube and a white microcrystalline solid was deposited in the bottom of the tube (presumably $NaBPh_4$ and NaCl). The dark blue crystals were collected and dried in vacuo. Yield: 0.12 g (37%). Anal. Calcd for $C_{50}H_{42}N_8B_1S_2V_1\cdot CH_2Cl_2$: C, 63.46; H, 4.56; N, 11.60. Found: C, 62.85; H, 4.47; N, 11.88. IR (KBr disk, cm^{-1}): 3419, 3104, 3054, 1578, 1500, 1466, 1400, 1276, 1202, 1106, 1064, 987, 871, 805, 743, 703, 627, 612, 464.6.

$[Co(L1)_2][BPh_4]$, 3. L1 (0.20 g, 7.298 × 10^{-4} mol), NaOMe (0.0394 g, 7.298 × 10^{-4} mol), and $NaBPh_4$ (0.125 g, 3.649 × 10^{-4} mol) were dissolved in MeCN (10 cm^3) forming a yellow solution. To this solution was added anhydrous $CoCl_2$ (0.0474 g, 3.649 × 10^{-4} mol) which instantly dissolved, causing the color of the solution to change to a deep emerald green. The reaction mixture was stirred for 30 min at room temperature, during which time a small amount of a white microcrystalline solid (NaCl) deposited. The solution was then filtered to remove the white solid and the filtrate evaporated to dryness under a reduced pressure yielding a deep green glass. The glass was dissolved in CH_2Cl_2 (10 cm^3) and EtOH (10 cm^3) was added. The solution was allowed to stand and slowly evaporate for several days during which time green blocky crystals of the product were deposited. The crystals were then collected by filtration, washed with EtOH (2 cm^3), and dried in vacuo. Yield: 0.087 g (27%). Anal. Calcd for $C_{50}H_{42}N_8B_1Co_1S_2\cdot CH_2Cl_2$: C, 62.94; H, 4.52; N, 11.51. Found: C, 63.18; H, 4.30; N, 11.76. IR (KBr disk, cm^{-1}): 3396, 3101, 3051, 2990, 1581, 1561, 1510, 1470, 1444, 1409, 1368, 1287, 1211, 1180, 1104, 1069, 1003, 871, 830, 805, 733, 708, 627, 612.

$[Co(L1)_2][BF_4]\cdot 2H_2O$, 3a. L1 (0.20 g, 7.298 × 10^{-4} mol) was dissolved in MeOH (15 cm^3). To this solution was added $Co(BF_4)_2.6H_2O$ (0.124 g, 3.649 × 10^{-4} mol) which instantly dissolved causing the solution color to change to brown. The reaction mixture was refluxed for 2 h during which time the solution underwent a further color change to deep green and a microcrystalline green solid precipitated. This solid was collected by the filtration of the hot mother liquor, and the solid washed with MeOH (5 cm^3) and dried in vacuo. The green product was recrystallized by layering a MeCN solution of the complex with $^iPr_2O$. Over a period of several days green plate crystals were deposited, which were collected and dried in vacuo. Yield: 0.12 g (48%). Anal. Calcd for $C_{26}H_{22}N_8B_1Co_1F_4S_2\cdot 2H_2O$: C, 45.1; H, 3.75; N, 16.2; Co, 8.5. Found: C, 44.42; H, 3.20; N, 15.42; Co, 8.91. IR (KBr disk, cm^{-1}): 3242, 3121, 3008, 1619, 1578, 1552, 1516, 1474, 1457, 1412, 1375, 1280, 1210, 1070, 894, 871, 832, 809, 751, 739, 688, 658, 629, 605, 522, 459.

$[Fe(L1)_2][ClO_4]$, 4. L1 (0.20 g, 7.298 × 10^{-4} mol) was dissolved in MeOH (10 cm^3) forming a very pale yellow solution. To this solution was added $Fe(ClO_4)_3\cdot 10H_2O$ (0.169 g, 3.649 × 10^{-4} mol) which quickly dissolved causing the solution to change to a slightly deeper yellow color but otherwise no other indications of reaction were observed. Triethylamine was then added dropwise to the solution at 30 s intervals between drops. After each drop a small amount of brown solid was deposited which quickly redissolved, with an associated color change in the solution to deep green. By the third drop of triethylamine, a dark green microcrystalline solid was deposited in the reaction mixture which was collected by filtration, washed with MeOH (4 cm^3), and dried in vacuo. Yield: 0.11 g (44%) Anal. Calcd for $C_{26}H_{22}N_8Cl_1Fe_1O_4S_2$: C, 46.88; H, 3.31; N, 16.83. Found: C, 46.61; H, 3.30; N, 16.98. IR (KBr disk, cm^{-1}): 3422, 2117, 2997, 1577, 1545, 1512, 1462, 1452, 1409, 1284, 1207, 1087, 984, 864, 831, 810, 750, 678, 629, 472.

Caution! *Metal perchlorates are potentially explosive.*

Crystallography. Dark blue plate crystals of $[V(L1)_2][BPh_4]\cdot MeCN\cdot {}^iPr_2O$ suitable for crystallographic investigation were grown by layering a MeCN solution of the complex with $^iPr_2O$. Green block crystals of $[Co(L1)_2][BPh_4]\cdot CH_2Cl_2$ of crystallographic quality were grown by layering a CH_2Cl_2 solution of the complex with hexane. Crystals of both $[V(L1)_2][BPh_4]\cdot MeCN\cdot {}^iPr_2O$ and $[Co(L1)_2][BPh_4]\cdot CH_2Cl_2$ were sealed in thin-walled quartz glass capillaries to prevent loss of lattice solvent to which they were prone. The crystals were mounted on a Siemens P4 diffractometer with a sealed-tube Mo X-ray source (λ = 0.710 73 Å) and controlled by Siemens XSCANS 2.1 software.

Table 2. Bond Distances (Å) for $[V(L1)_2][BPh_4]\cdot MeCN\cdot {}^iPr_2O$ and $[Co(L1)_2][BPh_4]\cdot CH_2Cl_2$

	V	Co
M1−S1	2.324(4)	2.250(1)
M1−S2	2.316(3)	2.255(1)
M1−N1	2.128(8)	1.965(3)
M1−N3	2.122(8)	1.924(3)
M1−N5	2.111(8)	1.973(3)
M1−N7	2.080(8)	1.936(3)

Table 3. Bond Angles (deg) for $[V(L1)_2][BPh_4]\cdot MeCN\cdot {}^iPr_2O$ and $[Co(L1)_2][BPh_4]\cdot CH_2Cl_2$

	V	Co
S1−M1−S2	97.2(1)	80.0(1)
S2−M1−N1	169.5(3)	175.9(1)
S2−M1−N3	89.2(2)	90.6(1)
S1−M1−N5	169.6(2)	176.4(1)
N1−V1−N5	84.5(4)	87.3(1)
S1−M1−N7	88.8(3)	90.9(1)
N1−M1−N7	93.6(3)	89.9(1)
N5−M1−N7	83.0(4)	90.3(1)
S1−M1−N1	89.5(3)	96.1(1)
S1−M1−N3	95.4(2)	88.9(1)
N1−M1−N3	82.1(3)	90.5(1)
S2−M1−N5	90.0(2)	96.7(1)
N3−M1−N5	92.3(3)	89.9(1)
S2−M1−N7	94.6(3)	89.0(1)
N3−M1−N7	173.9(4)	179.6(1)

Automatic searching, centering, indexing, and least-squares routines were carried out for $[V(L1)_2][BPh_4]\cdot MeCN\cdot {}^iPr_2O$ and $[Co(L1)_2][BPh_4]\cdot CH_2Cl_2$ with at least 25 reflections in the range $25 \leq 2\theta \leq 20°$ used to determine unit cell parameters. During data collection, the intensities of three representative reflections were monitored every 97 reflections but in no case was any serious decay observed. The data were corrected for Lorentz and polarization effects and for $[Co(L1)_2][BPh_4]\cdot CH_2Cl_2$ a semiempirical absorption correction was applied using ψ scan data. Structure solutions for $[V(L1)_2][BPh_4]\cdot MeCN\cdot {}^iPr_2O$ and $[Co(L1)_2][BPh_4]\cdot CH_2Cl_2$ were obtained by direct methods, and refinement by difference Fourier synthesis was accomplished using the Siemens SHELXTL-PC[24] software package. A summary of cell parameters, data collection conditions, and refinement results is given in Table 1. Selected bond lengths and angles are found in Tables 2 and 3. Details pertinent to the individual refinements are outlined below.

$[V(L1)_2][BPh_4]\cdot MeCN\cdot {}^iPr_2O$. This structure was solved by direct methods, revealing one $[V(L1)_2]^+$ cation and one $[BPh_4]^-$ anion in the asymmetric unit. Subsequent isotropic refinement revealed the presence two molecules of lattice solvent in the asymmetric unit, one of MeCN and one of $^iPr_2O$. All the non-hydrogen molecules were refined anisotropically except for the boron atom of the $[BPh_4]^-$ anion and the lattice solvent molecules which were refined isotropically. Due to the relatively small amount of observed data a 2σ cutoff was used and the phenyl rings of the $[BPh_4]^-$ anion were refined as rigid bodies to reduce the number of parameters. The hydrogen atoms were included in the final cycles of refinement in calculated positions using a riding model with fixed isotropic thermal parameters.

$[Co(L1)_2][BPh_4]\cdot CH_2Cl_2$. The solution of this crystal structure by direct methods indicated the presence of one $[Co(L1)_2]^+$ cation, one $[BPh_4]^-$ anion, and one molecule of lattice CH_2Cl_2 within the asymmetric unit. Isotropic refinement indicated that the solvent CH_2Cl_2 molecule was disordered over two positions. The two CH_2Cl_2 fragments were therefore weakly constrained to have similar C−Cl bond lengths, and occupancy factors were refined, giving 0.726 for the major position and 0.274 for the minor. All the non-hydrogen atoms in the structure were refined anisotropically. In the final cycles of refinement hydrogen atoms were included in calculated positions using a riding model with fixed isotropic parameters, except for the lattice CH_2Cl_2 solvent molecule for which no hydrogen atoms were included.

(24) Sheldrick, G. M. *SHELXTL-PC*, Version 4.1; Siemens X-ray Analytical Instruments, Inc.: Madison, WI, 1989.

Scheme 1

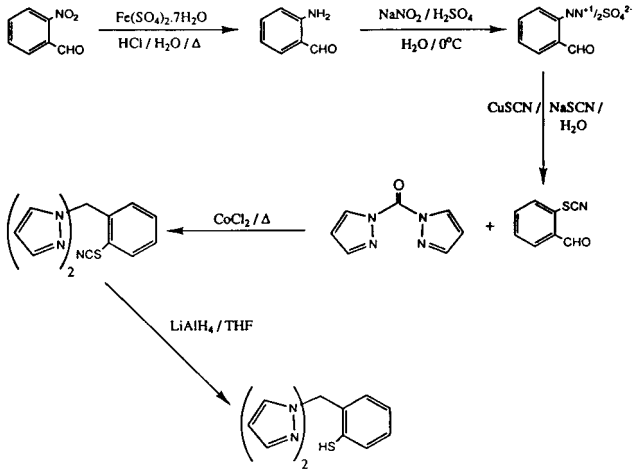

Results

Ligand Synthesis. The synthetic strategy we developed to synthesize the N_2S_{thiol} donor ligand, (2-thiophenyl)bis(pyrazolyl)methane, is summarized in Scheme 1. The synthesis consists of five steps; the first three are concerned with producing a suitable aldehyde starting material (2-thiocyanatobenzaldehyde) which can be reacted with bis(pyrazolyl)ketone to form a ligand precursor which can easily be converted into the active thiol ligand. The synthesis of 2-thiocyanatobenzaldehyde was accomplished via the method described by West et al.[23] However, rather than converting the 2-thiocyanatobenzaldehyde to the 2-thiobenzaldehyde directly, it was considered a better strategy to react the former with the bis(pyrazolyl)-ketone due to the high reactivity of the free thiol group in 2-thiobenzaldehyde. Thus the thiocyanato group was left in place as an effective protecting group for the thiol, thereby avoiding the problems inherent in using the highly reactive 2-thiobenzaldehyde. Although the reported hydroxide ion cleavage of the thiocyanato group of the (2-thiocyanatophenyl)-bis(pyrazolyl)methane was unsuccessful with yields of less than 5%, the much more vigorous conditions employed using $LiAlH_4$ cleanly cleaved the thiocyanato group in yields as high as 85%.

Metal Complex Synthesis. The metal(III) complexes described herein can be made by two general procedures starting either with a M(II) precursor followed by oxidation or directly from a M(III) salt. Which method works best depends on the metal in question. The Co(III) derivative for example is prepared by reaction of cobalt(II) tetrafluoroborate with the ligand in methanol. This initially forms a Co(II) linear trimer[25] which rapidly oxidizes in the air to produce the desired CoL_2^+ species. For vanadium, direct reaction of VCl_3 with 2 equiv of the ligand in the presence of base leads directly to the V(III) complex. Finally for Fe(III) the product can be produced starting with either Fe(III) or Fe(II) although the former gives the purer product.

Description of Structures. $[V(L1)_2][BPh_4]\cdot MeCN\cdot {}^iPr_2O$. The asymmetric unit of the crystal structure of this complex contains four discrete groups: one $[V(L1)_2]^+$ cation, one $[BPh_4]^-$ anion, one lattice solvent MeCN molecule, and one $^iPr_2O$. The $[V(L1)_2]^+$ cation (Figure 1) contains two L1 ligands coordinated to one V^{3+} metal atom in a tripodal, tridentate manner resulting in a V^{3+} coordination number of 6. The V^{3+} stereochemistry can best be described as slightly distorted

(25) Higgs, T. C.; Carrano, C. J. *Inorg. Chem.* **1998**, submitted.

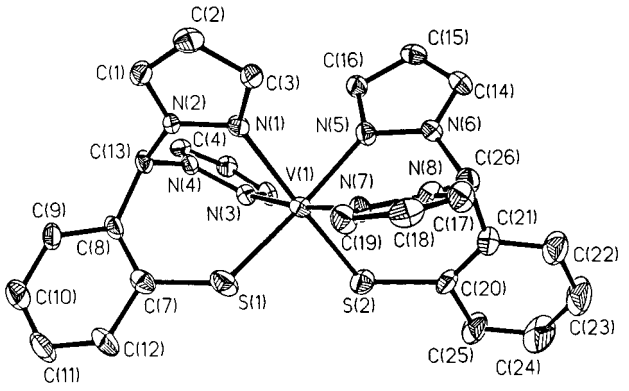

Figure 1. ORTEP view of the $[V(L1)_2]^+$ cation of **2** with 30% probability ellipsoids and atomic labeling. A corresponding ORTEP view with atomic labeling for the $Co(L1)_2^+$ cation of **3** is given in Supporting Information.

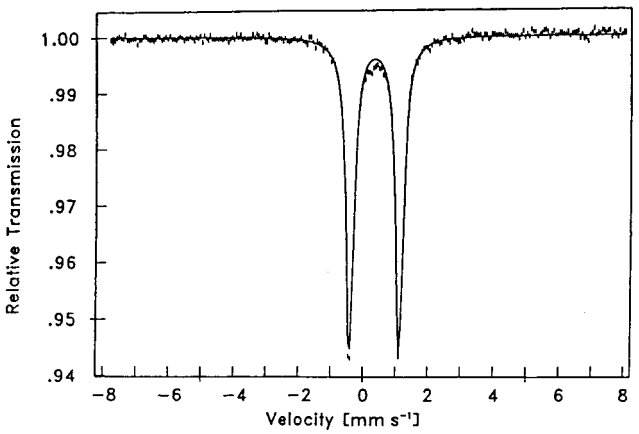

Figure 2. 77 K Mossbauer spectrum of solid **4** in zero applied field.

octahedral with the S_{thiol} donors oriented cis to each other with a non bonded S···S separation of 3.479 Å. The S1−V1−S2 bond angle of 97.1(1)° exhibits considerable expansion from the "ideal" octahedral value of 90°. This accordingly compresses the opposite (within the S1, S2, N1, N5 plane) "cis" N1−V1−N5 angle to a value of 84.5(4)°. The two L1 intraligand, N1−V1−N3 and N5−V1−N7 bond angles are also highly compressed to values of 81.9(3) and 83.2(4)°, respectively. Two factors contribute to the observed compression: the relatively small fixed "bite" size of L1 ligand and the length of the V1−N_{pz} bonds (average = 2.111 Å). Within the S1, S2, N1, N5 plane, the two L1 intraligand S1−V1−N1 and S2−V1−N5 bond angles of 89.5(3) and 90.1(3)°, respectively, have values very close to "ideal" octahedral values due to the larger size and greater flexibility of the seven-membered $N_2C_4S_1V_1$ chelate rings. The V−S and V−N bond lengths (V−S_{av} = 2.321 Å; V−N_{av} = 2.111 Å) are consistent with those expected for these ligand donor atoms and trivalent vanadium.

$[Co(L1)_2][BPh_4]\cdot CH_2Cl_2$. The asymmetric unit of the crystal structure of this complex contains three groups: one $[Co(L1)_2]^+$ cation, one $[BPh_4]^-$ anion, and one lattice solvent CH_2Cl_2 molecule. The $[Co(L1)_2]^+$ cation again contains two L1 ligands coordinated to one Co^{3+} metal atom in a tripodal, tridentate fashion making the Co^{3+} atom of the complex 6-coordinate. The Co^{3+} stereochemistry is again slightly distorted octahedral with the S_{thiol} donors orientated cis to each other with a S···S separation of 2.896 Å. This value differs considerably from that observed in the $[V(L1)_2]^+$ cation (3.479 Å) being almost 0.5 Å shorter. The S1−Co1−S2 bond angle is thus considerably compressed from the ideal value to an angle of 80.0(1)°. The two $N_2C_1Co_1$ ring-chelated L1 intraligand N−Co1−N pyrazole angles are effectively ideally octahedral with values of 90.5(1)° for N1−Co1−N3 and 90.3(1)° for N5−Co1−N7, in contrast to the compressed values observed in the $[V(L1)_2]^{2+}$ cation. This is due to the Co1−N_{pz} bond lengths being considerably shorter (average = 1.949 Å) than those of the $[V(L1)_2]^{2+}$ cation (average V1−N_{pz} = 2.111 Å), which effectively pulls the Co^{3+} atom further into the L1 ligand "pocket" causing a corresponding increase in all of the L−Co−L bond angles. Otherwise the ligand parameters (e.g. ligand "bite" size and pyrazole/phenyl ring orientation) are very similar in both complexes.

The Co−S and Co−N bond lengths for the $[Co(L1)_2]^+$ cation (Co−S_{av} = 2.253 Å; Co−N_{av} = 1.949 Å) are consistent with those expected for these ligand donor atoms and low-spin Co(III). Close examination of the Co−N_{pz} bond lengths indicates that there is a elongation of approximately 0.04 Å (the structural trans influence) of the two Co−N_{pz} bonds that are trans to the S_{thiol} ligands (Co1−N1 = 1.965(3) Å; Co1−N5 = 1.973(3) Å) compared to the two N_{pz} ligands that are cis to the two S_{thiol} (Co1−N7 = 1.936(3) Å; Co1−N3 = 1.924(3) Å).

Magnetic Resonance Spectroscopy. Room-temperature solid-state magnetic measurements on the deep green Fe(III) complex gave a μ_{eff} of 2.83 μ_B. This is slightly larger than that expected (normal 1.9−2.3 μ_B) for the single unpaired electron of low-spin Fe(III) even with the relatively large orbital contribution inherent in the T_{2g} ground state, suggesting a possible equilbrium with a *small* amount of high spin Fe(III) at room temperature. However at low temperature the exclusive presence of the low-spin configuration was indicated by both EPR and Mossbauer spectroscopy. In the solid state at 10 K, **4** showed a single broad isotropic signal with a g value of 2.117. No trace of a feature at $g = 4.3$ characteristic of high-spin Fe(III) in a rhombic environment was seen either at 10 or 77 K. In frozen solution (acetonitrile/toluene) at 77K a somewhat more anisotropic but still poorly resolved spectrum was observed with approximate rhombic "g" tensors of 2.32, 2.12, and 1.93, typical of low-spin Fe(III).[26] The values reported for nitrile hydratase are 2.27, 2.14, and 1.97.[6]

Low-temperature (77 K) Mossbauer spectroscopy of solid **4** is also consistent with the low-spin nature of the iron and displays a simple unsplit quadrupole doublet with an isomer shift of 0.345 mm/s and a quadrupole splitting of 1.529 mm/s (Figure 2). At the same temperature active nitrile hydratase is reported[27] to have an isomer shift of 0.33 and quadrupole splitting of 0.37 mm/s, the latter parameter of which is very different from **4** and reflects a more symmetrical electric field gradient at the iron nucleus. This suggests a high degree of back-donation of electron density from the protein ligands rendering the iron more "ferrous-like" than is seen in the known model complexes. This is likely due more to the presence of the unusual peptide nitrogen donors than the thiolates.[28]

NMR of the diamagnetic Co analogue, **3**, clearly shows that the "cis" stereochemistry present in the solid state is maintained in solution as well since in the "cis" geometry the two pyrazole rings of the ligand become inequivalent with one being trans to the thiolate sulfur and the other trans to another pyrazole while a plane of symmetry is expected for the trans isomer. Complete spectral assignments are given in Supporting Information and were made using a combination of COSY and HETCOR techniques.

(26) Sakurai, H.; Tsuchiya, K.; Migita, K. *Inorg. Chem.* **1988**, *27*, 3879.
(27) Honda, J.; Teratani, Y.; Kobayashi, Y.; Nagamune, T.; Sasabe, H.; Hirata, A.; Ambe, F.; Endo, I. *FEBS Lett.* **1992**, *301*, 177.
(28) Collins, T. J. *Acc. Chem. Res.* **1994**, *27*, 279.

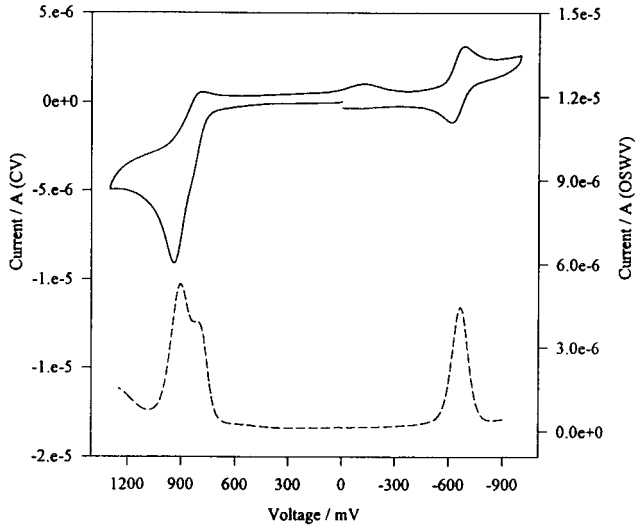

Figure 3. Electrochemistry of **2** in acetonitrile. Upper trace, cyclic voltammetry at 200 mv/s; lower trace, Osteryoung square wave voltammetry (conditions as described in the text).

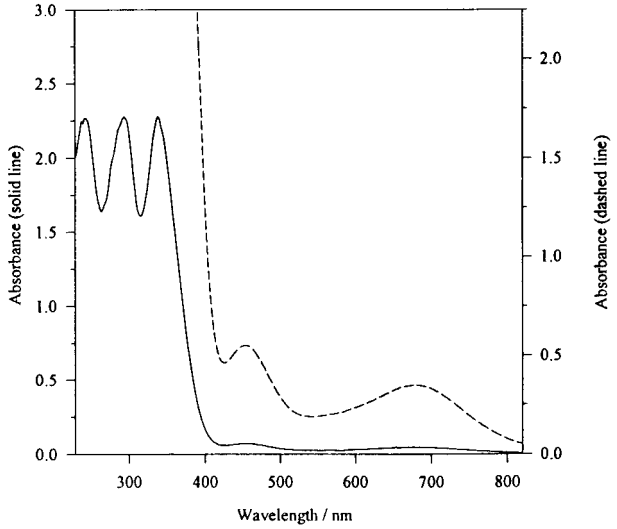

Figure 4. Optical spectrum of **3** in acetonitrile.

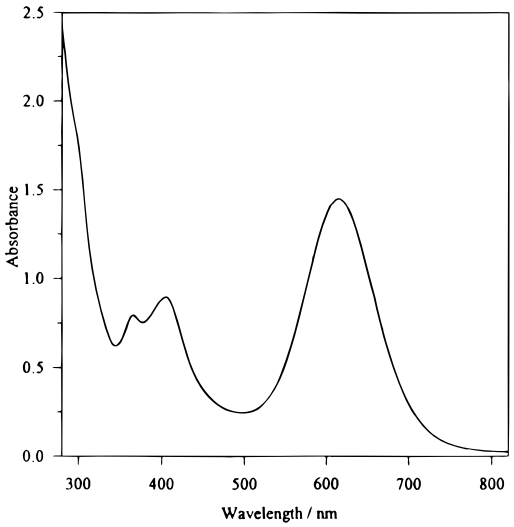

Figure 5. Optical spectrum of **2** in acteonitrile.

Electrochemistry. Cyclic voltammetry (CV) was performed on both the Co(III) and V(III) complexes; the Fe(III) species was insufficiently stable in solution for detailed study. The CV for the V(III) complex is shown in Figure 3. It is characterized by a quasireversible feature at −0.66 V assigned as the $V^{3+} \rightarrow V^{2+}$ reduction along with an irreversible wave at +0.90 V which is due to ligand oxidation. A product wave appears at ca. −0.10 V after scanning through the peak at +0.9 V. A more careful examination of the feature at +0.9 V reveals the presence of a shoulder which suggests that a metal-based oxidation is being obscured by the ligand electrochemistry. Using Osteryoung square wave voltammetry the second oxidation at +0.79 V is clearly revealed (Figure 3b) and is assigned as the quasireversible oxidation of $V^{3+} \rightarrow V^{4+}$. The situation for Co(III) is similar. Here a somewhat less reversible reduction of $Co^{3+} \rightarrow Co^{2+}$ appears at −0.38 V and the irreversible ligand oxidation at +0.92 V. A second irreversible oxidation is also observed at +1.05 V which we assign as the oxidation of $Co^{3+} \rightarrow Co^{4+}$. The ligand itself shows no electrochemistry within the potential limits of +1.5−1.5 V thus the feature assigned as ligand oxidation at +0.9 V in both the vanadium and cobalt complexes likely represents the oxidation of the coordinated sulfurs to disulfide.

Optical Spectroscopy. The Fe(III) complex forms a deep green solution in acetonitrile with relatively intense bands at 492 and 724 nm (see Figure 9) very similar to the spectrum reported for the iron nitrile hydratase.[2] While it is not possible to report accurate extinction coefficients for this species due to its rapid decomposition in solution, it can be estimated to be in the range of 1−2000 M^{-1} cm^{-1} at 724 nm based on a linear extrapolation to zero time. Thus the 724 nm band is clearly LMCT in character, presumably due to a S → Fe transition (vide infra). At first glance the spectrum of the cobalt complex is similar with relatively weak bands at 454 nm (609 M^{-1} cm^{-1}) and 678 nm (385 M^{-1} cm^{-1}) and two intense ones (17000 M^{-1} cm^{-1}) at 338 and 294 nm (Figure 4). The bands in the visible region could be either relatively weak LMCT transitions or d−d in origin, in which case the intensities have been increased either by borrowing from an intense band in the near UV or from some sort of symmetry reduction. Resonance Raman spectroscopy seems to preclude the former description (vide infra). On the other hand, if we assume that the two bands represent the $^1A_{1g} \rightarrow {}^1T_{1g}$ and $^1A_{1g} \rightarrow {}^1T_{2g}$ transitions expected for a strong-field d^6 system in a pseudooctahedral field then standard ligand field calculations predict a value for $10D_q$ of 15 128 cm^{-1} which would mean that the ligand field is weaker even than fluoride which gives a high-spin complex! This is obviously unrealistic, hence we assign the two bands in the visible region as due to a splitting of the $^1A_{1g} \rightarrow {}^1T_{1g}$ transition engendered by a lowering of the symmetry from O_h.[29] The two intense bands in the near-UV are then assigned as S → Co CT transitions (they cannot be ligand-based transitions since they do not appear in the V^{3+} analog) which is reasonable both from literature precedence and on the basis Jorgenson's optical electronegativity theory (vide infra).[30,31] It is perhaps significant that two bands seen at 304 and 331 nm have been speculated to be S→Co CT transitions in the cobalt containing nitrile hydratase from *Pseudomonas putida.*[32]

The V(III) complex (Figure 5) displays a rich spectrum with an intense band at 616 nm (6436 M^{-1} cm^{-1}) and two somewhat weaker features at 364 (3527 M^{-1} cm^{-1}) and 406 nm (3984 M^{-1} cm^{-1}). All these transitions clearly derive from S → V

(29) Gahan, L. R.; Hughes, J. G.; O'Connor, M. J.; Oliver, P. J. *Inorg. Chem.* **1979**, *18*, 933.
(30) Jorgenson, C. K. *Mol. Phys.* **1963**, *6*, 43.
(31) Patch, M. G.; Carrano, C. J. *Inorg. Chim. Acta* **1981**, *56*, L71.
(32) Payne, M. S.; Wu, S.; Fallon, R. D.; Tudor, G.; Stieglitz, B.; Turner, I. M.; Nelson, M. J. *Biochemistry* **1997**, *36*, 5447.

CT given the high extinction coefficients observed and the resonance Raman results.

A theoretical basis for the assignment of the S → M CT bands can be obtained from the optical electronegativity theory of Jorgenson.[30,31] Details can be found in the cited references, but the equation below has been found to correlate the transition energies of LMCT bands for a wide range of metal ions and ligands:

$$\nu_{corr} = 30(\chi_L - \chi_M)$$

where χ_L and χ_M are the optical electronegativities of the ligand and metal respectively, and ν_{corr} is the transition energy of the first allowed LMCT transition corrected for interelectronic repulsion and ligand field effects. Using the known values of optical electronegativity for the trivalent metals[31] and for thiolate donors,[33] along with reasonable values for ligand field parameters as appropriate, one predicts that the lowest energy S → M CT bands should appear at 767 nm for low-spin Fe(III), 636 nm for V(III), and ca. 333 nm for Co(III), in quite good agreement with the observed values.

Resonance Raman Spectroscopy. Resonance Raman (RR) spectroscopy has proven to be a useful tool for the exploration of the active sites of metallosulfur enzymes where the enzyme exhibits a S → M^{n+} charge-transfer band.[34] We have therefore investigated the RR spectra of **2**−**4** both as an aid in the assignment of their optical spectra and for comparison with the Fe and Co nitrile hydratase enzymes. All of the compounds in this study display very similar bands near 1586, 1555, 1290, and 1036 cm^{-1} in the high-frequency region, which are characteristic of the thiophenol portion of the ligand. Metal-insensitive bands near 380, 440, and 470 cm^{-1} also appear to derive from the ligands. However, bands in the range of 300−350 cm^{-1} exhibit different frequencies with the different metals, and this suggests that these bands arise from the M−S stretches. Furthermore it is expected that the two M−S motions in these cis dithiolates should be coupled to one another since the noncoupling requirement could only be met if the coordination shell of the metal were so rigid that the metal ion could not be displaced by excitation into higher M−S vibration modes.[35] Assuming the S−M−S unit to have rough C_{2v} symmetry one would expect both in-phase (symmetric) and out-of-phase (antisymmetric) stretches. Thus, the two metal-sensitive peaks in the 300−350 cm^{-1} range are presumed to the symmetric and asymmetric S−M−S stretches. Accordingly, the bands at 312 and 333 cm^{-1} in **3** are attributed to Co−S vibrations (Figure 6). The single-crystal X-ray structure shows that the Co−S bond length is similar to that of the Cu−S distance in bis(thiosemicarbazonato)Cu^{II},[36] for which a Raman band at 330 cm^{-1} has been assigned to the Cu−S stretch.[37] Badger's rule[38] then predicts that they both should have the same force constant of 1.39 mdyn/Å. A simple calculation for an isolated Co−S oscillator with this force constant gives a frequency of 337 cm^{-1}, which is comparable to the observed value of 333 cm^{-1}. The band at 312 cm^{-1} is assigned to the symmetric Co−S mode, while the band at 333 cm^{-1} is assigned to the asymmetric Co−S mode, since the polarization experiment demonstrates that the band at 312 cm^{-1} is polarized (data not shown). Although the symmetric mode is normally expected to be at higher energy and to be more intense than the antisymmetric one, coupling between the Co−S and ligand modes caused by the acute S−Co−S angle cause an upshift of the asymmetric stretch. The excitation profile for **3** (Figure 7) indicates that the relative intensity of the 312 cm^{-1} peak with respect to the 986 cm^{-1} of internal standard K_2SO_4 is tremendously enhanced in the near-UV region. This confirms the assignment of the absorption band at 338 nm as being due to S → Co CT transition with the bands at 450 and 680 nm likely being of d−d origin.

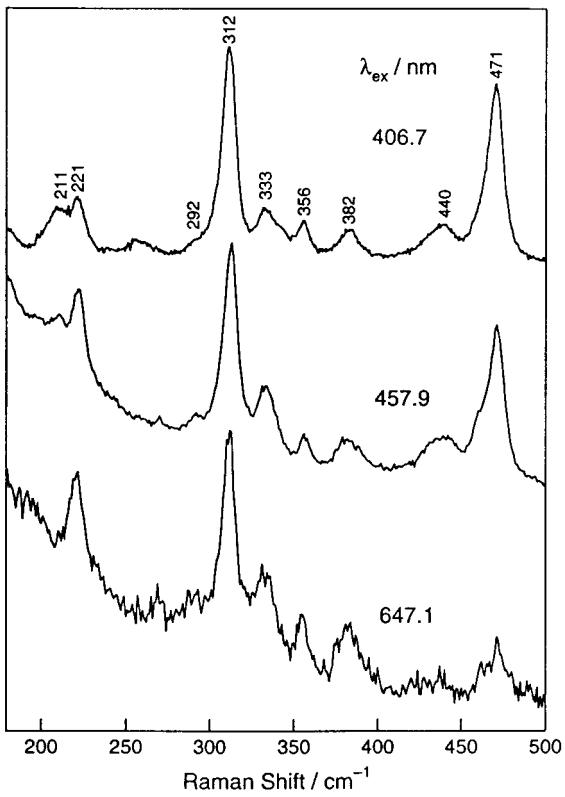

Figure 6. Resonance Raman spectra of solid **3** with 406.7 (top), 457.9 (middle), and 647.1 nm (bottom) excitation wavelengths, 150 mW laser power, and 6 cm^{-1} slit width.

The similarity in the RR spectra between Fe and Co suggests that the structures of the two are not significantly different. The band at 325 cm^{-1} is therefore assigned to the asymmetric Fe−S mode, while the band at 315 cm^{-1} is assigned to the symmetric Fe−S mode (Figure 8). However, the definitive polarization experiment for the Fe−thiolate was not possible due to its rapid decomposition in solution. This assignment also confirms the low-spin configuration for the Fe(III) in **4** since low-spin Fe−S stretching vibrations are reported to be found in the 300−340 cm^{-1} range while the corresponding vibrations for the high-spin state are found between 210 and 240 cm^{-1}.[39] The excitation profile for **4** (Figure 9) indicates the band at 325 cm^{-1} is enhanced under red light excitation, which is consistent with the suggestion that the absorption band at 720 nm is one with substantial S → Fe charge-transfer (CT) character. That the band at 315 cm^{-1} is strongly enhanced with violet light excitation indicates that the shoulder at 344 nm in the optical spectrum of **4** is also due to a S → Fe CT transition, similar to that at 338 nm in the Co complex.

(33) Thompson, J. S.; Sorrell, T.; Marks, T. J.; Ibers, J. A. *J. Am. Chem. Soc.* **1979**, *101*, 4193.
(34) Andrew, C.; Sanders-Loehr, J. *Acc. Chem. Res.* **1996**, *29*, 365.
(35) Brennen, B. A.; Cummings, J. G.; Chase, D. B.; Turner, I. M.; Nelson, M. J. *Biochemistry* **1996**, *35*, 10068.
(36) Taylor, M. R.; Glusker, J. P.; Gabe, E. J.; Minkin, J. A. *Bioinorg. Chem.* **1974**, *3*, 189.
(37) Tosi, L.; Garnier-Suillerot, A. *J. Chem. Soc., Dalton Trans.* **1982**, *1*, 103.
(38) Herschbach, D. R.; Laurie, V. W. *J. Chem. Phys.* **1961**, *35*, 458.
(39) Hutchinson, B.; Neill, P.; Finkelstein, A.; Takemoto, J. *Inorg. Chem.* **1981**, *20*, 200.

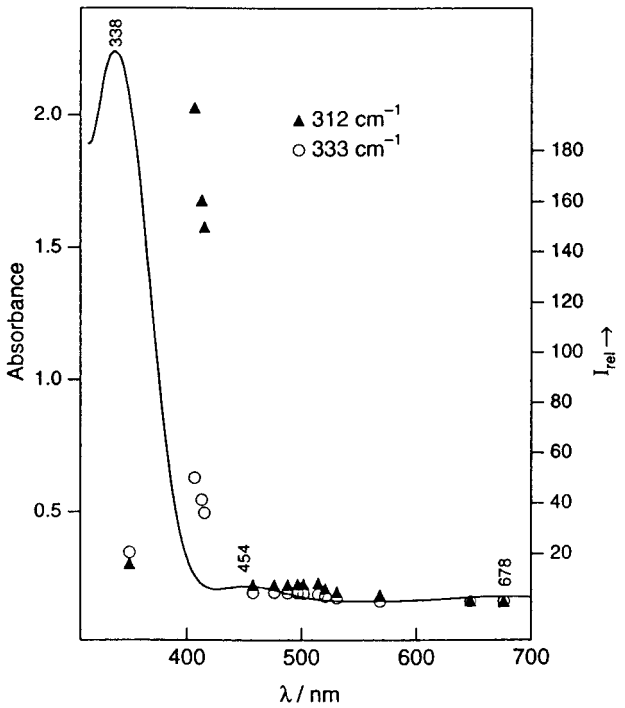

Figure 7. Excitation profiles for the 312 and 333 cm^{-1} ν(Co−S) modes of **3**.

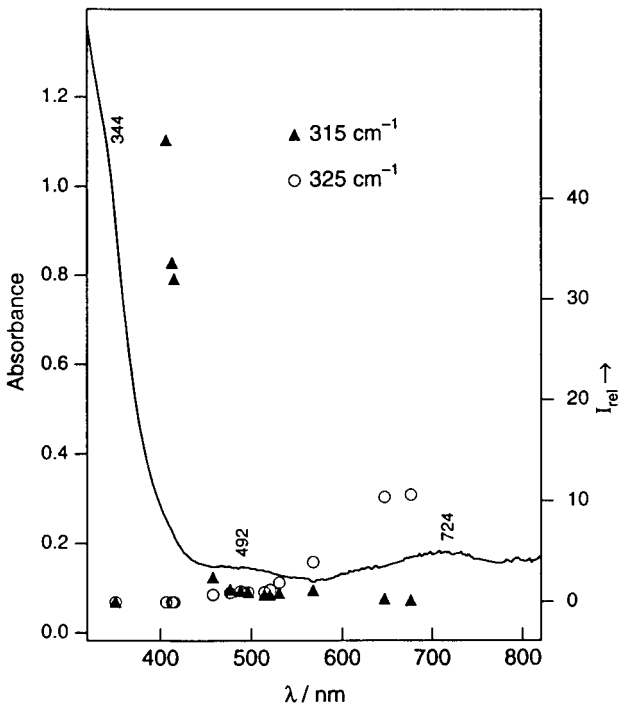

Figure 9. Excitation profile for the 315 and 325 cm^{-1} ν(Fe−S) modes of **4**.

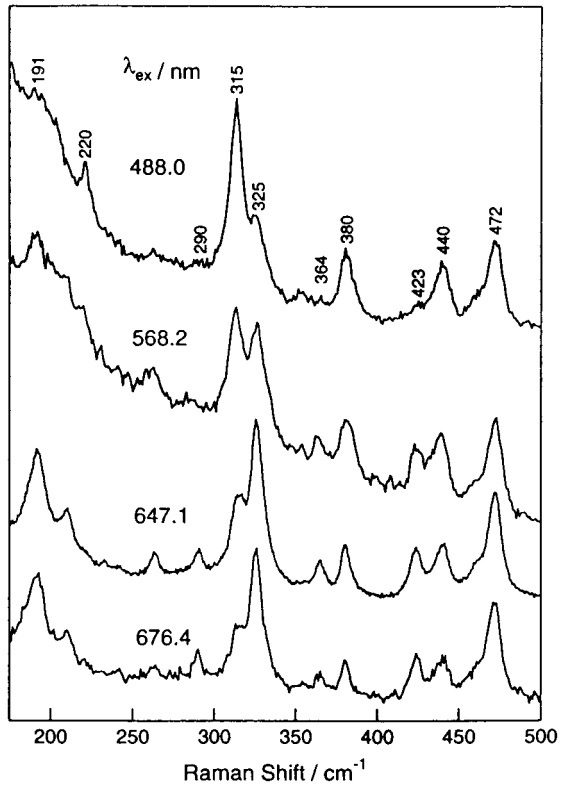

Figure 8. Resonance Raman spectra of solid **4** (conditions as described for Figure 6).

In recent studies, Spiro and others have proved that the coupling of the C−CH_2−S modes to the metal−sulfur vibrations are significant in the RR spectra of metal−cysteinate proteins.[40,41] Indeed the plethora of bands in the range expected for M−S vibrations for the nitrile hydratase and other metal sulfur enzymes such as the blue copper proteins is attributed to this kinematic coupling between the M−S stretch and cysteine−ligand deformations (such as the S−C−C bend).[35] Isotopic studies show that none of the enzyme bands are pure Fe−S stretches but that many of them have significant M−S character.[35] Since the aromatic thiolates in **4** do not display the kinematic coupling, direct comparison of the model compound and the enzyme is futile. However, it can be said that the ligand bands for Co and Fe in this region are nearly identical, which indicates similar structures.

The Raman spectrum of the vanadium complex **2** is distinctly different (Figure 10) from that of the Co and Fe analogues. Bands at 303 and 319 cm^{-1} in **2** are tentatively assigned to the V−S stretching frequencies. Assuming that the band at 303 cm^{-1} is the symmetric stretch and using a simple triatomic oscillator model, we predict that the asymmetric stretch should come at a frequency of 318 cm^{-1}, very close to the 319 cm^{-1} actually seen. Measurements (data not shown) indicate that the band at 303 cm^{-1} is enhanced in the red region, as is a ligand band at 469 cm^{-1}. Thus the absorption band at 616 nm has significant S → V CT character. On the other hand, the enhancement of 303 cm^{-1} under violet excitations also suggests the absorption band at 406 nm to be a S → V charge transfer as well. However, the polarization experiment shows that these two bands are both polarized, and this implies that these bands are not pure V−S stretches but arise from the coupling to other modes as well.

Discussion

Mossbauer and EPR spectroscopy both clearly show that the Fe in **4** is low spin. Resonance Raman spectroscopy is also consistent with this view.[39] This is surprising given that the vast majority of Fe(III) complexes are high spin. The factors contributing to this strong ligand field remain somewhat obscure.

(40) Qiu, D.; Kilpatrick, L.; Kitajima, N.; Spiro, T. G. *J. Am. Chem. Soc.* **1994**, *116*, 2585.

(41) Nestor, L.; Larrabee, J. A.; Woolery, G.; Reinhammar, B.; Spiro, T. G. *Biochemistry* **1984**, *23*, 1084.

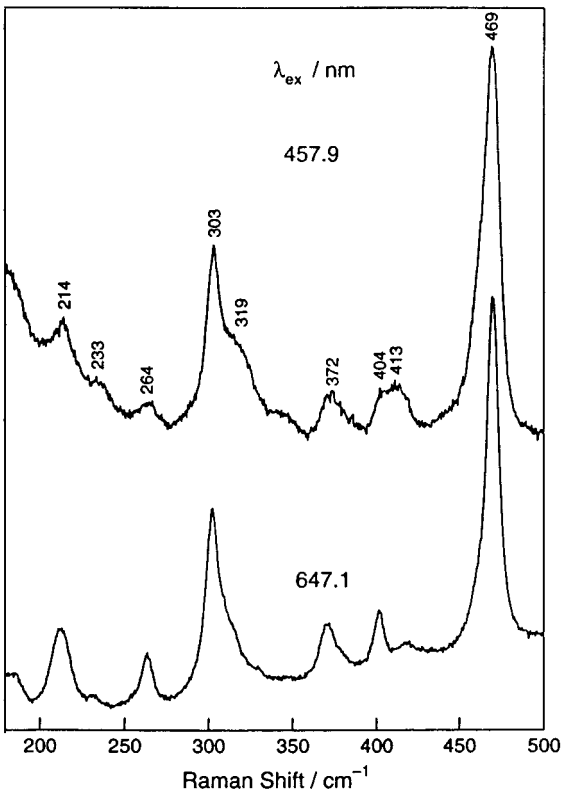

Figure 10. Resonance Raman spectra of solid **2** with 457.9 (top) and 647.1 nm (bottom) excitation (other conditions as in Figure 6).

However, the number of sulfur donors may prove to be decisive since complexes with S_6 or N_3S_3 donor spheres appear to be either high spin or in spin equilibrium while those with the N_4S_2 environment described here are largely low spin. Kovacs et al. have pointed out the "ambiguous" nature of the ligand field strength of sulfur as a donor and suggested that a delicate balance related to the number of sulfur donors may be a critical factor in achieving a low-spin environment.[15] Our results are certainly in accord with such an idea. In the nitrile hydratase enzyme where the iron is known to be low spin, the spin state may be more a result of the presence of the very strong field amide nitrogens than the presence of the three thiolate donors.[28]

While we have been unable to determine the X-ray structure for the iron complex due to its instability in solution, we presume that its structure is analogous to that of the vanadium and cobalt analogues, **2** and **3**, and that the stereochemistry is therefore "cis". This is based not only on the observation of only "cis" stereochemistry in both the Co^{3+} and V^{3+} complexes but on the similarity between the IR and resonance Raman spectra of all three species. This stereochemistry is unexpected since for a facially coordinating ligand with sulfur donors such as L1, simple steric arguments would have suggested the "trans" arrangement to be the more stable. However, if π back-bonding between the sulfurs and the metal is important, as appears likely given the observed structural trans influence, then the cis geometry should be preferred to avoid competion for the electron density in the same metal orbitals which would be engendered by the trans arrangement.[42]

One result of the apparent preference for the cis geometry may be found in the structural evidence for an apparent S···S interaction. While a cursory inspection of the V^{3+} and Co^{3+} complexes reveal them to be very similar "cis-sandwich"

Scheme 2

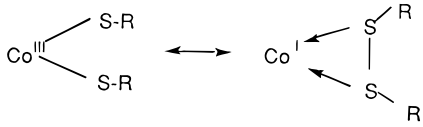

Table 4. Redox Potentials in Acteonitrile for Vanadium Complexes of the Type $(pz)_2XHY$ Where X = C or B and Y = Thiophenol, Phenol or Pyrazole

X	Y	$V^{3+} + e^- \rightarrow V^{2+}$	$V^{3+} \rightarrow V^{4+} + e^-$	ref
C	thiophenol	−664 mV	+800 mV	this work
C	phenol	−1112 mV	+1060 mV	this work
B	pyrazole	−420 mV		44

species, more detailed analysis reveals a remarkable and unexpected difference. Although both complexes contain pseudooctahedrally coordinated metal, there is a major difference in the "nonbonded" S···S distance between the cis sulfurs and in the corresponding S−M−S angle. In the case of the cobalt derivative the S···S distance is a relatively short 2.896 Å (sum of the covalent radii = 2.04 Å), while in the vanadium derivative it is 3.479 Å. In addition the S−M−S angle in the former is acute at 80° but obtuse (97°) in the latter. While some of these differences can be attributed to the difference in size between the Co^{3+} and V^{3+} ions leading to shorter Co−L bonds, this can by no means explain the 0.6 Å shorter S···S distance or the 17° more acute S−M−S angle. Thus it appears that for cobalt at least a resonance form such as that shown on the right in Scheme 2 contributes significantly to the overall electronic structure. Such resonance forms have been suggested to be important to the chemistry of Mo−thiols in molybdoproteins.[43] One is tempted to suggest that the instability of the iron complex in solution is also due to a predominance of the resonance form on the right which leads to reduced metal and oxidized (disulfide) ligand. Such an idea is supported by the similarity in the resonance Raman spectra between Fe and Co. However, the lack of a crystal structure leaves this notion unproved.

One of the major advantages of the new class of "heteroscorpionate" ligands of which the thiolate, L1, is a member is that they allow a systematic comparison of spectroscopic and electronic properties of metal complexes with similar or identical topology that vary only in the nature of one of the donor atoms. Redox potentials represent a good example of these trends. A comparison of the redox potentials of the V(III) complexes of the tris(pyrazolyl)borate,[44] (2-thiophenyl)bis(pyrazolyl)methane, and (2-hydroxyphenyl)bispyrazolylmethane are illustrative. The V(III) complexes generally show both one-electron reductions to V(II) as well as one-electron oxidations to V(IV), the potentials of which vary with the nature of the donor (Table 4). The all-N donor sphere provides, as expected, the most stabilization of the V(II) oxidation state (i.e. it is the easiest to reduce) followed by the thiolate with the phenolate by far the hardest to reduce. The overall difference on going from an N_6 to N_4S_2 to N_4O_2 donor sphere is ca. 0.7 V. On the oxidative side, the pattern is that the vanadium thiolate is easiest to oxidize followed by the phenolate and then by far the hardest is the all-N analogue. This pattern illustrates the dual nature of the sulfur donors which can stabilize both high and low oxidation states. Data such as this may be useful in estimating changes in metalloprotein properties upon site directed mutagenasis of one set of amino acid donors for another.

(42) Elder, R. C.; Florian, L. R.; Lake, R. E.; Yacynych, A. M. *Inorg. Chem.* **1973**, *12*, 2690.

(43) Barnard, K. R.; Bruck, M.; Huber, S.; Grittini, C.; Enemark, J. H.; Gable, R. W.; Wedd, A. G. *Inorg. Chem.* **1997**, *36*, 637.

(44) Mohan, M.; Holmes, S. M.; Butcher, R. J.; Jasinski, J. P.; Carrano, C. J. *Inorg. Chem.* **1992**, *31*, 2029.

Finally we come to the question of how kinetically inert metal ions can function as centers for enzymatic reactions. A number of published reports indicate that some types of sulfur coordination to Co(III) induce remarkable effects on the *kinetics* of ligand substitution trans to the sulfur donor.[45] The *structural* trans influence such as the one we describe here is significant only with anionic thiolate donors and not for example with formally neutral thioethers. In turn thioethers do not show any trans labilizing influence. Thus for Co(III) at least there is evidence that correlates the "kinetic trans effect" with the "structural trans influence", caused by a lengthening (and hence presumably weakening) of the bonds trans to sulfur.[42] It should be pointed out, however, that the relationship between the structural trans influence and the kinetic trans effect for metals other than Co(III) is by no means a direct or trivial one. The cobalt complex reported here clearly shows the structural trans influence, with the pyrazole nitrogen donors trans to the thiolates, some of which are 0.04 Å longer than those trans to another nitrogen. The magnitude of this structural trans influence is also similar to that previously reported and suggests that a kinetic labilization of the trans positions could be operative. What does this tell us about how formally inert metals can function in an enzyme? Although the mechanism of action of neither the iron nor the cobalt nitrile hydratase enzymes is known at this time, two broad possibilities exist. The nitrile substrate can coordinate directly to the metal center, occupying what appears to be the open axial site.[5] A nitrile coordinated to a strong Lewis acidic metal ion such as Fe(III) or Co(III) would be expected to be polarized to make it more susceptible to nucleophilic attack by water to yield product. The axial site, being trans to a thiolate donor, is expected to be relatively labile to ligand exchange allowing substrate binding and product release. Alternatively the nitrile substrate, rather than being directly bound to the metal, is held nearby to what might be expected to be a labile water or hydroxide bound in the open axial position.[46] Such a metal-coordinated species is expected to be a better nucleophile than free water or hydroxide. While the above is clearly speculative, it does provide a basis for understanding how fundamentally kinetically inert metal ions can be modified by ligation to function in labile enzymatic centers.

Acknowledgment. This work was supported by Grants AI-1157 (to C.J.C.) and E-1184 (to R.S.C.) from the Robert A. Welch Foundation. The NSF-ILI Program Grant USE-9151286 is acknowledged for partial support of the X-ray diffraction facilities at Southwest Texas State University.

Supporting Information Available: NMR spectral assignments for **3** and complete list of atomic positions, bond lengths and angles, anisotropic thermal parameters, hydrogen atom coordinates, data collection, and crystal parameters and ORTEP diagrams for **2** and **3** (18 pages). Ordering information is given on any current masthead page.

IC971151E

(45) Elder, R. C.; Kennard, G. J.; Payne, M. D.; Deutsch, E. *Inorg. Chem.* **1978**, *17*, 1296.

(46) Jin, H.; Turner, I. M.; Nelson, M. J.; Gurbiel, R. J.; Doan, P. E.; Hoffman, B. M. *J. Am. Chem. Soc.* **1993**, *115*, 5290.